Short communication

# Composite organic radical–inorganic hybrid cathode for lithium-ion batteries

Qian Huang, Lelia Cosimbescu, Phillip Koech, Daiwon Choi, John P. Lemmon*

*Pacific Northwest National Laboratory, 908 Battelle Boulevard, P.O. Box 999, Richland, WA 99354, USA*

## HIGHLIGHTS

► Organic radical–inorganic hybrid cathode comprised of PTMA/LiFePO₄ is developed.
► Hybrid cathode shows the enhanced electrochemical performances.
► Hybrid cathode demonstrates significant improvement in high pulse power performance.

## ARTICLE INFO

## ABSTRACT

A new organic radical–inorganic hybrid cathode comprised of poly(2,2,6,6-tetramethylpiperidinyloxy-4-yl methacrylate) (PTMA)/LiFePO$_4$ composite system was developed and reported for the first time. The hybrid electrodes' voltammetry contains three pairs of reversible redox peaks indicating the combination of electrochemical characteristics between LiFePO$_4$ and PTMA electrodes and shows a decrease in voltage gap between oxidation and reduction that corresponds to an improvement in the rate and reversibility of the redox couples. Results from electrochemical impedance spectroscopy show lower charge-transfer resistance of cycled hybrid cathodes suggesting an enhanced electrode/electrolyte interface formed in hybrid systems which leads to faster migration of Li ions through the interface and longer cycle life capability when compared with pure LiFePO$_4$ or PTMA cathode system. Optimizing the hybrid cathode's ratio of PTMA/LiFePO$_4$ yields a significant improvement in high pulse power performance (30 mAh cm$^{-3}$) over the pure PTMA (16 mAh cm$^{-3}$) or LiFePO$_4$ (3.0 mAh cm$^{-3}$) cathode. Further characterization of the hybrid electrodes using SEM showed a more compact surface morphology after high rate pulse experiments. The demonstrated properties of hybrid cathodes are promising for transportation and other high pulse power applications that require long cycle life and low cost.

© 2013 Published by Elsevier B.V.

## 1. Introduction

Since the first successful commercialization in 1991, lithium-ion batteries have been widely used as power sources in portable electric devices and more recently large-scale applications that include transportation and smart grid integration due to their acceptable electrochemical performances and cycle life [1–4]. In current Li-ion batteries, the cathode is the main limiting factor in energy density and capacity. The conventional cathode material is inorganic based, lithium transition-metal oxide, which is charged or discharged electrochemically by de-intercalation or intercalation of the lithium ions [5]. This charge transfer mechanism has led to batteries with relatively high energy density and long cycle life at low to moderate current rates. However during high current charge or discharge excursions, mass transfer limitations and other factors increase the cell over-potential that leads to subpar energy densities along with increased cell temperatures limiting cycle life and safety [6–8]. The decrease in cycle life significantly impacts the overall cost of electrochemical storage when using a $kWh/cycle metric. Decreased performance affecting battery efficiency along with, cycle life, safety, cost, as well as other issues related to materials toxicity and resource availability are the primary barriers to widespread adoption of lithium based batteries in hybrid and full electric vehicles [3].

Another class of electrochemical energy storage materials is organic polymers such as conductive, redox active (i.e. carbonyl and sulfur based) and stable radical polymers [9,10]. Polymers that feature an organic radical moiety as the energy storage species are attractive as cathode candidates for Li-ion batteries due to their relatively high discharge voltage (vs. Li/Li$^+$) [11] and gravimetric

capacity which has been recently found in our research. In particular, radical polymers containing a robust unpaired electron nitroxide radical group have demonstrated reversible electrochemical redox reactions in aprotic solutions [12,13]. The fast reaction mechanism results in high power capability with the added benefit of environmentally friendly materials and polymer like materials properties (elastic, light weight). However, similar to other polymer energy storage systems they possess low (volumetric) energy density that has limited their use beyond research and thin film application.

To improve the state-of-art lithium battery performance and cycle life, we propose the organic radical–inorganic hybrid cathode concept to achieve high power performance from the organic radical moiety while maintaining the high volumetric energy density from the inorganic. In this paper, we demonstrate the benefits of a new hybrid cathode comprised of poly(2,2,6,6-tetra-methylpiperidinyloxy-4-yl methacrylate) (PTMA)/LiFePO$_4$ composite system that provides improved electrochemical performances over pure PTMA or LiFePO$_4$ cathode that are capable of high pulse power performance and stability, resulting in longer cycle life and lower cost.

## 2. Experimental

### 2.1. Preparation of organic radical–inorganic hybrid electrode

The PTMA, synthesized following a procedure published by Nakahara et al. [12], was used as the organic radical electrode-active material; and the LiFePO$_4$ (Phostech Lithium, Sud-Chemie) was used as the inorganic electrode-active material. The electrode was prepared by paper electrode making process using Ketjen black (KB) as conductive and PTFE as binder [14]. To obtain organic radical–inorganic hybrid electrodes while maintaining an optimized electrode environment for each component, these two distinct materials were combined by introducing the compositions of entire PTMA electrode (16.7% PTMA, 73.3% KB, and 10% PTFE) and the entire LiFePO$_4$ electrode (80% LiFePO$_4$, 10% KB, and 10% PTFE) with different weight ratios of 25/75, 50/50, and 75/25 in the hybrid electrodes, marked as hybrid 1–3 respectively.

### 2.2. Cell preparation and electrochemical measurements

The working electrode, with a surface area of 1.6 cm$^2$ and thickness of 0.2–0.3 mm, was assembled into a half-cell configuration (2325 coin-type) in a dry glove box by using Li metal as an anode, 1 M LiPF$_6$ in ethyl carbonate/dimethyl carbonate (1:1) as an electrolyte, and Celgard 3501 membrane as a separator. The cells were electrochemically cycled using an Arbin BT-2000 Battery Tester at room temperature. The high rate pulse discharge (HRPD) protocol followed the procedures: charging galvanostatically at the 1C rate with the cutoff potentials of 4.2 V vs. Li/Li$^+$; and discharging at the 1C rate for 60 s followed by 10C (high rate pulse) for 6 s, repeating 1C and 10C with the cutoff potentials of 2.0 V vs. Li/Li$^+$ where the cell was then recharged. The C rate is based on the theoretical capacity of 200 mAh g$^{-1}$ for PTMA, and 168 mAh g$^{-1}$ for LiFePO$_4$ as active material respectively. The cyclic voltammetry (CV) and electrochemical impedance spectroscopy (EIS) of the cells were carried out using a Solartron workstation. The CV measurement was performed with the low scan rate of 0.1 mV s$^{-1}$ and the potential range of 4.5–2.0 V vs. Li/Li$^+$ for five cycles. The EIS measurement was performed over a frequency range of 10 mHz to 100 kHz with a perturbation voltage of 5 mV, and the cells were tested at around 3.0 V vs. Li/Li$^+$ (OCV) before and after five charge–discharge cycles. The surface morphology of fresh electrodes and the electrodes after HRPD cycling was detected by using

a focus ion beam-scanning electron microscope (FEI Helios 600 Dual Beam).

## 3. Results and discussion

### 3.1. Electrochemical characterizations

The electrochemical performances of hybrid electrodes have been investigated by cyclic voltammetry (CV) and electrochemical impedance spectroscopy (EIS). For comparison, pure PTMA or LiFePO$_4$ electrode has also been characterized. Fig. 1 shows the CV curves of Li/LiFePO$_4$, Li/PTMA, and Li/hybrid-(1–3) cells at a scan rate of 0.1 mV s$^{-1}$ between 2.0 and 4.5 V vs. Li/Li$^+$ for the first and fifth cycles. The curve (a) of LiFePO$_4$ electrode shows one pair of reversible peak at 3.82 V (anodic) and 3.03 V (cathodic), attributed to the lithium ion de-intercalating from and intercalating into the olivine phase of Li$_x$FePO$_4$ respectively.

The curve (b) of PTMA electrode presents two pairs of reversible redox peaks indicating a two-electron redox reaction of the nitroxide radical (shown in the scheme of curve b) [15,16]. The first pair at 3.68 V (anodic) and 3.57 V (cathodic) with the difference of separation of 0.11 V corresponds to the reaction between the organic radical (OR) and oxoammonium cation (p-type); and the second pair at 3.13 V (anodic) and 3.03 V (cathodic) with the difference of 0.10 V corresponds to the reaction between the OR and aminoxy anion (n-type). In both cases charge neutrality is maintained by the ions from the electrolyte salt. The voltammetry of PTMA electrode indicates three unique advantages as an energy storage material: 1) fast electrode reaction kinetics indicated by the small gap of the anodic and cathodic peaks, suggesting a high (pulse) power capability in a cycled battery [12]; 2) a high theoretical capacity achieved by two-stage redox reaction from a cation (p-type) via a radical to an anion (n-type), which has rarely been observed in lithium-ion batteries [17]; and 3) a notable effect of (pseudo)electric double layer capacitance disclosed by a rectangular shape area of CV curve (excluding two pairs of redox peaks) [17,18], that is around 58% of total area of CV curve. Here the enhanced electrochemical properties of PTMA electrode may be associated with the introduction of high surface area carbon (KB) [19] as a conductive medium that enhances electronic conductivity of electrodes through the formation of an extensive electron percolation network. Our results indicate that the carbon network promotes the two-electron transfer behavior and super-capacitor related property of PTMA electrode. A detailed investigation of the PTMA radical and mechanism related to energy storage will be discussed in our future work.

The hybrid electrodes' voltammetry is comprised of three pairs of redox peaks I–III in curve (c) that indicates the combination of electrochemical characteristics between LiFePO$_4$ and PTMA electrodes: the large pair of redox peaks (I) in the range of 3.2–3.7 V is attributed to the lithium ion insertion/extraction through Li$_x$FePO$_4$; and two pairs of smaller peaks (II–III) in the ranges of 2.8–2.9 V and 3.6–3.7 V (the anodic peak III is overlapped by the anodic peak I) are attributed to the two-electron redox reaction behavior of PTMA. Moreover when compared to pure PTMA and LiFePO$_4$ electrode profiles, the hybrid electrodes show shifts in the oxidation and reduction voltage that is dependent on the ratio of PTMA/LiFePO$_4$. Also observed is the sharper redox peaks compared to pure electrodes and the decrease in voltage gap between oxidation and reduction with the increase in PTMA/LiFePO$_4$ ratio from 25/75 to 75/25, indicating improvement in the rate and reversibility of the redox couples.

The CV results of hybrid electrodes are associated with the influence of electrode environments. As described in the Experimental, the hybrid electrode combines the compositions of
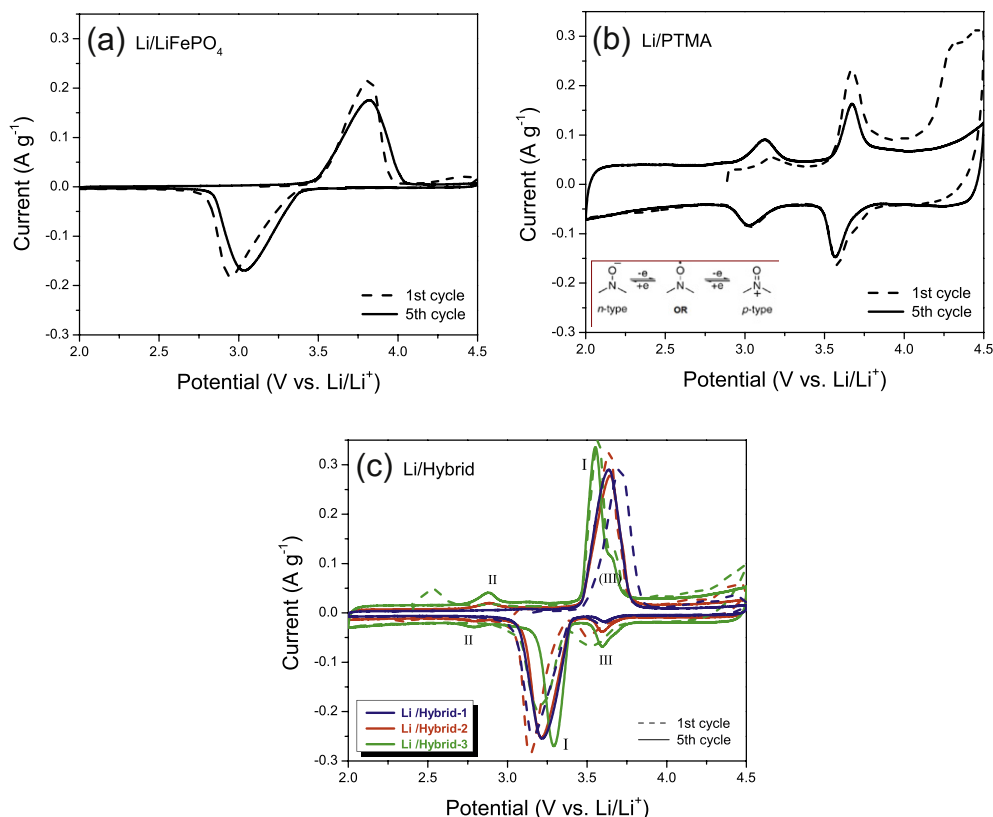
**Fig. 1.** Cyclic voltammetry curves of five cells: (a) Li/LiFePO₄, (b) Li/PTMA, and (c) Li/hybrid-1, Li/hybrid-2, and Li/hybrid-3 with the PTMA/LiFePO₄ ratios of 25/75, 50/50, 75/25 in hybrid electrodes respectively, at scan rate 0.1 mV s⁻¹ and potential range 4.5–2.0 V vs. Li/Li⁺ for the first and fifth cycles.

PTMA electrode and LiFePO₄ electrode with different weight ratios, where the PTMA electrode contains a much higher loading of conductive carbon (73.3% KB) than the LiFePO₄ electrode (10% KB) due to PTMA's highly insulating characteristics. The composition of hybrid electrodes is the result of balancing two very different environments required for two different active materials. In the CV curves, the redox peaks observed from both active materials demonstrate that hybrid electrodes significantly maintain the original environment for each component; meanwhile the shifts and reshaping of the hybrid redox peaks suggest a different charge transfer environment compared with pure PTMA and LiFePO₄ electrodes. This indicates the local environments from each active material might influence each other in the hybrid electrode, i.e. the electrode environment surrounding one active material may be shared by the other. Therefore with the increase in PTMA/LiFePO₄ ratio, the corresponding increase of conductive carbon (KB) to maintain the electrode environment of PTMA may enhance the electrode environment surrounding LiFePO₄ in hybrid electrodes. This could lead to a synergistic effect associated with the environment interactions between the PTMA radical and LiFePO₄, and such interaction may promote the charge transfer mechanism in the hybrid electrode system.

Electrochemical impedance spectroscopy (EIS) has also been explored here to characterize the electrode/electrolyte interface (solid electrolyte interface, SEI) property which is the key factor to the electrochemical stability and cycle life of Li-ion batteries. Fig. 2 shows the typical Nyquist plots of Li/LiFePO₄, Li/PTMA, and Li/hybrid-(1–3) cells at 3.0 V vs. Li/Li⁺ (OCV) before and after five charge–discharge cycles. Each curve is composed of a depressed semicircle in high- to middle-frequency regions and a line in low-frequency regions. As reported in the literature [20,21], the

intercept of real axis ($Z'$) at high frequency region corresponds to the resistance of electrolyte solution ($R_{sol.}$) and the one at low frequency region corresponds to the resistance of electrode/electrolyte interface and charge transfer ($R_f$). For the fresh electrodes, the values of $R_{sol.}$ are near zero and almost the same (2–5 Ω),
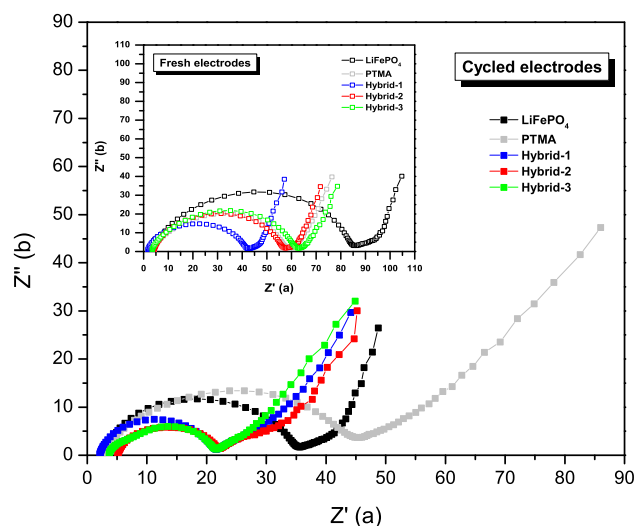


**Fig. 2.** Typical Nyquist plots by EIS spectra of Li/LiFePO₄ (black), Li/PTMA (gray), Li/hybrid-1 (blue), Li/hybrid-2 (red), and Li/hybrid-3 (green) cells with fresh electrodes (inset) and the electrodes after five cycles at the same voltage of 3.0 V, over a frequency ranges 100 kHz to 10 mHz, and perturbation voltage 5 mV. (For interpretation of the references to colour in this figure legend, the reader is referred to the web version of this article.)

which suggests high ionic conductivity of electrolyte in all five cells. And these values did not change after five cycles indicating no distinct reduction in ionic conductivity of electrolyte (or mobility of ions) with cycling of the cell. However, the values of $R_f$ vary for different cell systems. Li/LiFePO$_4$, Li/PTMA, and Li/hybrid-(1–3) cells show the $R_f$ values of 85, 60, and 42–63 $\Omega$ respectively for the fresh electrodes, and then decrease significantly to 35, 45, and around 22 $\Omega$ correspondingly after cycling. The decrease in $R_f$ indicates the formation of stable electrode/electrolyte interfaces [20,22] in all five cell systems. Note that all three hybrid cells show the nearly same $R_f$ after cycling and their values are much lower than that of pure LiFePO$_4$ or PTMA cell. These results indicate that an improved electrode/electrolyte interface has been formed in the hybrid cathode systems which leads to faster Li ion migration through the SEI layer and enhanced electrochemical properties when compared to pure LiFePO$_4$ or PTMA cathode system. The improved electrode/electrolyte interface properties can result in the high stability and long cycle life capability for hybrid cathodes which are promising for the practical applications of Li-ion batteries with low cost.

## 3.2. High pulse power performance

The electrochemical characterizations above (CV and EIS) demonstrate the capabilities of high (pulse) power and stability for hybrid electrodes. To validate these advantages, the cells were tested under high rate pulse discharge (HRPD) protocol measured by volumetric energy capacity (VEC). The HRPD protocol and VEC measurement were targeted for the practical applications of hybrid electrodes in transportation [23] or other high pulse power applications with limitations on volume. The protocol involves an initial charge at 1C rate to 4.2 V followed by discharge at 1C rate for 60 s followed by high rate (10 C) for 6 s. Such discharge cycle was repeated until the lower voltage limit of 2 V is reached. Fig. 3 shows the VEC for the 30 cycles of HRPD protocol. The Li/LiFePO$_4$ cell provides the highest volumetric energy capacity (96 mAh cm$^{-3}$) of all five cells for the initial charge at 1C, but rapidly decreases to 13.6 mAh cm$^{-3}$ for the first pulse discharge, and further decreases to around 3.0 mAh cm$^{-3}$ (the lowest value of the cells) after 30 continuous cycles of the HRPD protocol. These results demonstrate the mass transfer limitations of LiFePO$_4$ at high rate pulse excursions that can be partially attributed to the

intercalation based charge transfer mechanism of inorganic cathodes. The Li/PTMA cell shows the capacity of 17.4 mAh cm$^{-3}$ in the initial charge at 1C. When cycled using the HRPD protocol the capacity sustained around 16 mAh cm$^{-3}$ throughout the 30 cycles, demonstrating the high rate pulse capability indicative of the fast redox reaction mechanism identified in the CV curves. However, the overall volumetric capacity is pretty low for pure PTMA. The HRPD performance of the hybrid cells is highly dependent on the ratio of PTMA/LiFePO$_4$ in the composite electrode. The composite electrodes with the PTMA/LiFePO$_4$ ratios of 50/50 (hybrid-2) and 75/25 (hybrid-3) achieved much higher capacity (over 25 mAh cm$^{-3}$) than that of 25/75 (hybrid-1, about 10 mAh cm$^{-3}$) and maintain stable cycling throughout 30 continuous cycles of HRPD protocol. The best performance was obtained using a 50/50 PTMA/LiFePO$_4$ ratio (30 mAh cm$^{-3}$) that is significantly improved when compared to pure PTMA or LiFePO$_4$ electrode. The inset of Fig. 3 further displays the charge–discharge curves for the 5th, 15th, and 25th cycles of Li/LiFePO$_4$, Li/PTMA, and Li/hybrid-2 cells. As shown in the curves, the hybrid-2 electrode can sustain 10C pulse followed by 1C relaxation repeated for tens of times in one cycle of HRPD. According to our hypothesis for the organic radical–inorganic hybrid concept, the capacity in the high rate pulse process should be completely contributed by the organic radical moiety. But with this protocol, the observed capacity in the hybrid is much greater than the capacity that can be attributed by PTMA alone. Thus the hybrid electrode shows a synergistic effect beyond a simple physical mixture between the PTMA radical and LiFePO$_4$ on high rate pulse performance. This interaction probably promotes the fast charge transfer mechanism in the hybrid electrode system and is a subject of ongoing study in our laboratory.

Note that the hybrid electrode, by combining the compositions of PTMA electrode and LiFePO$_4$ electrode with different weight ratios, possesses the balanced loading of conductive carbon as aforementioned. For instance, the hybrid-2 electrode (with the PTMA/LiFePO$_4$ ratio of 50/50) has the conductive carbon KB loading of 41.7%, which is different from that of pure PTMA electrode (73.3%) and LiFePO$_4$ electrode (10%). In order to further validate the benefit of hybrid electrode, the cell performance for pure LiFePO$_4$ and PTMA electrodes with the same loading of each component as hybrid-2 electrode (48.3% active material, 41.7% conductive carbon, and 10% binder) was measured by VEC at low rate (0.1C), mid-rate (1C) and high rate (10C) pulse test, which is attached as Fig. S1 in the Supplementary data. It is found that the hybrid-2 electrode achieves higher capacity than pure electrodes with the same loading of conductive carbon throughout the whole cycles, demonstrating the significant improvement and synergistic effect in the hybrid electrode regardless of low rate, mid-rate, or even high rate pulse test.

Moreover, the surface morphology was characterized to better understand the electrochemical behaviors of hybrid electrodes. Fig. 4 shows the SEM images for hybrid-2, LiFePO$_4$ and PTMA electrodes before (fresh) and after HRPD. The image for hybrid-2 electrode shows the more uniform and compact film on the top surface of electrode after HRPD. This smooth film should be the enhanced electrode/electrolyte interface layer which has been well characterized in EIS measurement (Fig. 2). The formation of improved interface layer on the surface of hybrid electrode can effectively prevent the structure from degradation, which helps to the high pulse power performance and long cycle life. On the other hand, the rough and even grainless properties are observed on the surface of pure electrodes (especially for the LiFePO$_4$ electrode) after HRPD, which might have less protecting ability in high rate and long-term cycling. Thus these electrodes can not sustain the HRPD due to the damaged morphology, resulting in the poor performance ultimately.
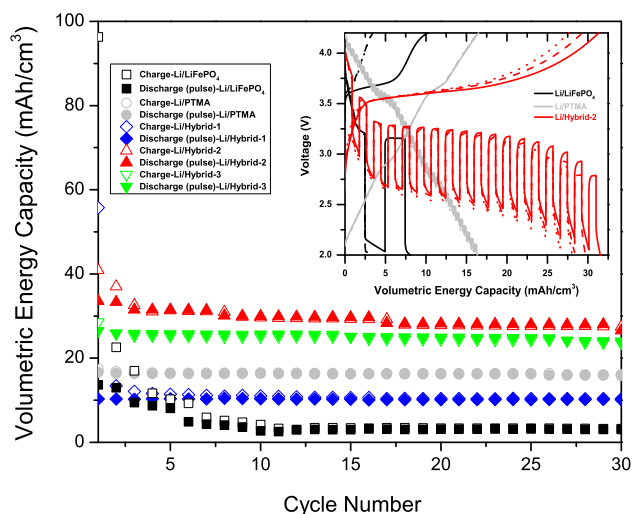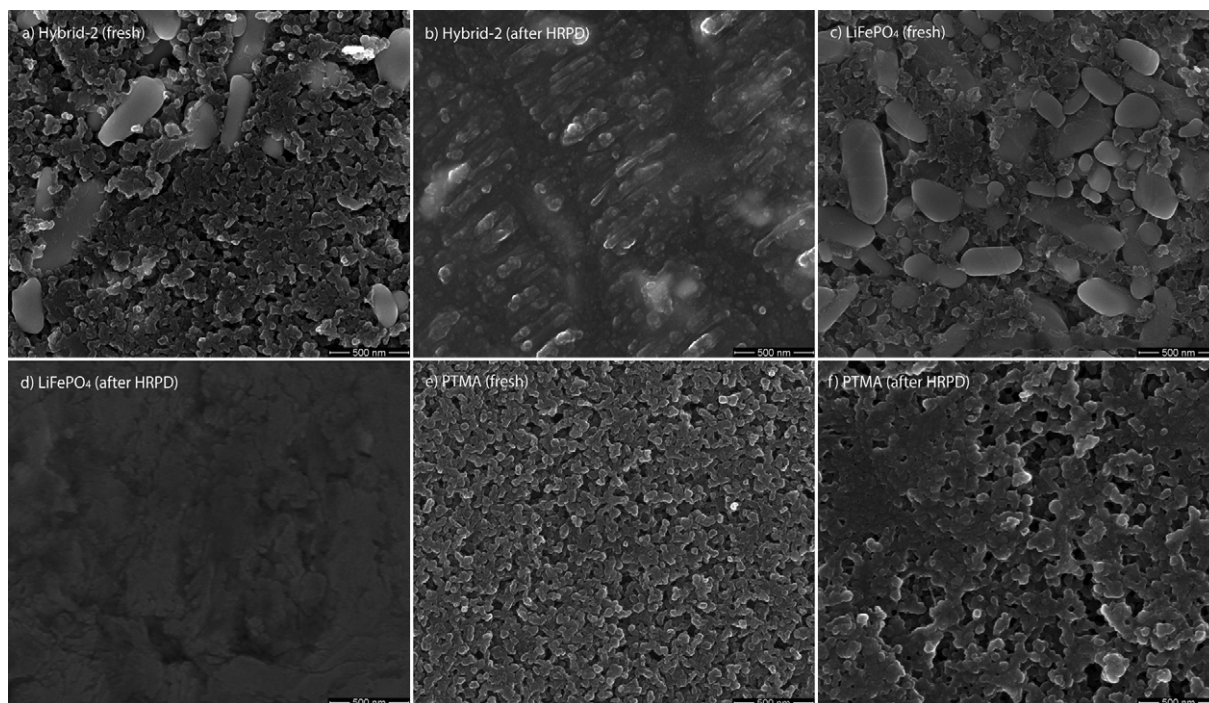


**Fig. 3.** Volumetric energy capacity (VEC) vs. cycle number in a high rate pulse discharge protocol for Li/LiFePO$_4$, Li/PTMA, and Li/hybrid-(1–3) cells. Inset: voltage vs. VEC for the 5th (solid line), 15th (dash line), and 25th (dot line) cycles.

**Fig. 4.** SEM images for the surface of fresh electrodes and the electrodes after high rate pulse discharge (HRPD) cycling: (a–b) for hybrid-2, (c–d) for LiFePO₄, and (e–f) for PTMA electrodes.

## 4. Conclusions

A new organic radical–inorganic hybrid cathode comprised of PTMA/LiFePO$_4$ composite system is developed and reported for the first time. The CV curves of hybrid electrodes are comprised of three pairs of redox peaks indicating the combination of electrochemical characteristics between LiFePO$_4$ and PTMA electrodes, and the decrease in voltage gap between oxidation and reduction demonstrates the improvement in the rate and reversibility of the redox couples. A lower charge-transfer resistance of cycled hybrid cathodes is determined by EIS suggesting an enhanced electrode/electrolyte interface formed in hybrid systems which lead to the much easier migration of Li ion through the interface and longer cycle life capability compared with pure LiFePO$_4$ or PTMA cathode system. Hybrid electrodes, by optimizing the ratio of PTMA/LiFePO$_4$, achieve the significant improvement in high pulse power performance over the pure PTMA or LiFePO$_4$ electrode. And the more compact surface morphology is observed in hybrid electrodes after high rate pulse by SEM characterization. Further mechanistic studies are currently ongoing. The demonstrated properties of hybrid cathodes are promising for transportation and other high pulse power applications that require long cycle life and low cost.

## Acknowledgments

## Appendix A. Supplementary data

Supplementary data related to this article can be found at http://dx.doi.org/10.1016/j.jpowsour.2013.01.076.

## References

[1] J.-M. Tarascon, M. Armand, Nature 414 (2001) 359.
[2] M. Wakihara, Mater. Sci. Eng. R 33 (2001) 109.
[3] B. Scrosati, J. Garche, J. Power Sources 195 (2010) 2419.
[4] Z. Yang, J. Zhang, M.C.W. Kintner-Meyer, X. Lu, D. Choi, J.P. Lemmon, J. Liu, Chem. Rev. 111 (2011) 3577.
[5] M.S. Whittingham, Chem. Rev. 104 (2004) 4271.
[6] N. Sato, J. Power Sources 99 (2001) 70.
[7] R. Spotnitza, J. Franklin, J. Power Sources 113 (2003) 81.
[8] Q. Huang, M. Yan, Z. Jiang, J. Power Sources 156 (2006) 541.
[9] P. Novak, K. Muller, K.S.V. Santhanam, O. Haas, Chem. Rev. 97 (1997) 207.
[10] Y. Liang, Z. Tao, J. Chen, Adv. Energy Mater. 2 (2012) 742.
[11] K. Nakahara, K. Oyaizu, H. Nishide, Chem. Lett. 40 (2011) 222.
[12] K. Nakahara, S. Iwasa, M. Satoh, Y. Morioka, J. Iriyama, M. Suguro, E. Hasegawa, Chem. Phys. Lett. 359 (2002) 351.
[13] H. Nishide, S. Iwasa, Y.-J. Pu, T. Suga, K. Nakahara, M. Satoh, Electrochim. Acta 50 (2004) 827.
[14] D. Choi, J. Xiao, Y.J. Choi, J.S. Hardy, M. Vijayakumar, M.S. Bhuvaneswari, J. Liu, W. Xu, W. Wang, Z. Yang, G.L Graff, J.-G. Zhang, Energy Environ. Sci. 4 (2011) 4560.
[15] E. Breuer, H.G. Aurich, A. Nielsen, Nitroenes, Nitronates and Nitroxides, John Wiley & Sons, New York, 1989.
[16] L.B. Volodarsky, V.A. Reznikov, Synthetic Chemistry of Stable Nitroxides, CRC Press, Florida, 1993.
[17] W. Guo, Y.-X. Yin, S. Xin, Y.-G. Guo, L.-J. Wan, Energy Environ. Sci. 5 (2012) 5221.
[18] W. Sugimoto, H. Iwata, Y. Yasunaga, Y. Murakami, Y. Takasu, Angew. Chem. Int. Ed. 42 (2003) 4092.
[19] J. Xiao, D. Wang, W. Xu, D. Wang, R.E. Williford, J. Liu, J.-G. Zhang, J. Electrochem. Soc. 157 (2010) A487.
[20] J.-K. Kim, G. Cheruvally, J.-W. Choi, J.-H. Ahn, S.H. Lee, D.S. Choi, C.E. Song, Solid State Ionics 178 (2007) 1546.
[21] S. Yoshihara, H. Isozumi, M. Kasai, H. Yonehara, Y. Ando, K. Oyaizu, H. Nishide, J. Phys. Chem. B 114 (2010) 8335.
[22] X.-Z. Liao, Z.-F. Ma, Y.-S. He, X.-M. Zhang, L. Wang, Y. Jiang, J. Electrochem. Soc. 152 (2005) A1969.
[23] (a USABC High Power Low Energy-Energy Storage System (LEESS) Goals (29 February 2012).(b Energy Storage System Goals: Power Assist HEV Battery Goals (12 October 2006);
(c EV Battery Test Procedures Manual (15 August 2006).http://www.uscar.org/guest/publications.php.